Correlated Percolating Networks in the Thin Film of Polymeric PEDT/PSS Complex As Revealed by the Mesoscale Simulation

Toomas Kaevand,[†] Jaan Kalda,[‡] Andres Öpik,[†] and Ülo Lille*[,†,†]

Department of Material Sciences, Tallinn University of Technology, Ehitajate tee 5, 19086 Tallinn, Estonia, and Institute of Cybernetics, Tallinn University of Technology, Akadeemia tee 21, 12618 Tallinn, Estonia

Received September 23, 2008
Revised Manuscript Received December 19, 2008

Introduction

Studies on the percolation behavior of ionomeric/polymeric systems are usually based on the relation between the volume fraction of respective active species and data on the mechanical properties, e.g.,[1] water and proton transport,[2] or supplied threshold value[3] (we refer the reader to the basics of the percolation theory presented in ref 4). Doped (oxidized) poly(3,4-ethylenedioxythiophene) (PEDT) stabilized with the counterionic poly(styrenesulfonic acid) (PSS) is one of the most studied conjugated polymers.[5] The structure and morphology of the thin films of the PEDT/PSS complex have been intensively investigated by various physical methods.[6−19] The electrical conductivity has been tentatively interpreted as the result of the presence of a percolating network of the coupled conducting particles. The hopping mechanism of conductivity is generally accepted.

However, there are only a few investigations on the relation of the morphology of the thin films with the properties at comparable conditions. This is because often the researchers have aimed at improving the properties of thin films through the modification of the preparation conditions.

Recently, the thin film of the PEDT/PSS complex has been imagined as a percolating conductor−insulator composite in which the conductor volume fraction is well above the percolation threshold.[20] This result has been deduced from the comparison of the data of XR and electrical conductivity measurements of pristine and water-washed films (the film thickness 65 and 42 nm, respectively). The water-washing increases the conductivity from 0.4 to 0.6 S/cm.

A natural question is, what is the percolation threshold value of such a system? It is also possible that there is no well-defined percolation threshold at all. Indeed, in the case of coupled conducting particles, strong long-range correlations are possible; at the limit of very strong correlations, the percolation threshold can disappear.[21] The present work aims at clarifying these questions.

As the experimental data are too scarce, we base our analysis on the density fields, generated in our investigation of the formation of the 3D morphology of the PEDT/PSS complex as a polyelectrolyte/ionomer[22] by the dynamic mean-field density functional theory.[23] This theory was implemented in a MesoDyn simulation code of the Material Studio program package (Accelrys, see the review on the mesoscale modeling of materials[24] as well).

After performing the cluster analysis of these fields, we are able to generate the percolation pathways and compare them in a pristine and water-washed thin films.

Methodology of the Calculations

The coarse-grained model of the chemically synthesized pristine PEDT/PSS associate system (PEDT to PSS mass ratio 1/2.5; doping level 0.25, as shown in ref 20) and the simulation parameters are described in detail in ref 22. In this report we use the statistical (random) copolymer model of an associated PSS chain (host charged, H_c). This mesomolecule is composed of an anionic and neutral sulfonate beads (denoted by Sc and Snc, respectively), at the ratio of 1 to 4, resulting in one Sc bead per four T beads. The neutral host (Hn) mesomolecule is a homopolymer consisting of Sn-type beads. The oligomeric G (guest) is formed from a single bead of type T (thiophene) assuming the delocalization of the doping-induced positive charge over all thiophene cycles. In the pristine associate system these three materials are present in equal volume percentage. The water-washed associate does not consist of Hn mesomolecules (the corresponding mass ratio 1/1.4). Thus, the coarse-grained model hopefully captures the essential morphological pattern of a molecular system consisting of about 10^8 atoms. As a result, all atomistic details are of course lost.

In the simulation process, the 3D morphology evolves according to the Langevin diffusion equations through the minimization of the free energy of the system (periodic boundary conditions are used). This results in the generation of the density (concentration) fields (ρ) of all beads in the simulation box of physical dimensions $82.3 \times 82.3 \times 82.3$ nm^3 discretized as a cubic grid of 32^3 cells. The density field of each bead spans from the maximum density (d_{max}) to zero. In the volume rendering conditions these fields are presented as the dimensionless volume fraction fields ($\eta = \nu\rho$, where ν is the bead volume, 2.275 nm^3).

The cluster analysis is based on the algorithm that selects only the cells having one side in common. First, we find such a minimal density d_c of the T cells that the largest cluster of cells with $d > d_c$ is percolating (i.e., touches a pair of opposite walls of the box). The ratio of the number of all the cells with $d > d_c$ to the net number of cells (32^3) plays the role of the critical probability p_c. In what follows, we also use the concept of "conduction window", which is the density interval $\Delta d = d_c - d_{max}$. It also makes sense to consider larger conduction windows, $\Delta d = (1 - y)d_{max} - d_{max}$. Then, the parameter y controls the size of the percolation clusters. Instead of y, one can use the respective probability p, i.e., the relative number of cells with $d > (1 - y)d_{max}$. We also determine the number of cells in the *percolation pathway* (i.e., in the infinite cluster) (N_p). This quantity includes the current-carrying core and "dead ends", i.e., the regions of the infinite cluster which are connected to the current-carrying core via one conducting cell only. The ratio of N_p to the total number of cells (N_p/N) is referred to as the density of the infinite percolating cluster $P(p)$. Analogously, the term $P(p)_b$ is defined as the ratio of N_b/N where N_b is the number of cells in the backbone.

Our intuitive reasoning on the conduction window is rather similar to that of the continuum percolation with a broad distribution of the conductivities.[4] This is in line with the

* Corresponding author. E-mail: lille@chemnet.ee.
† Department of Material Sciences.
‡ Institute of Cybernetics.

10.1021/ma802160x CCC: $40.75
Published on Web 01/21/2009

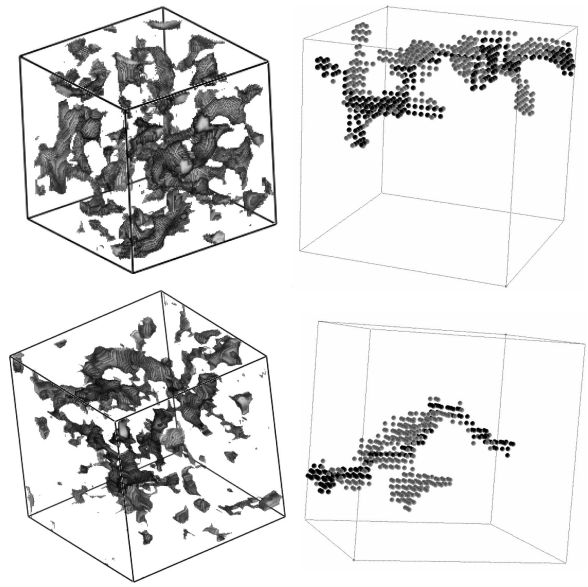

Figure 1. Conduction window of T beads in the pristine film, $\Delta d = 0.647 - 0.841$, and the respective percolation pathway (the upper row); the same for the water-washed film (the lower row), $\Delta d = 0.814 - 0.950$; the percolation pathways (gray dots) and backbones (black dots) are distinguished; the values of p_c and $P(p)/P(p)_b$ (in parentheses) 0.0802 (0.0210/0.00812) and 0.0632 (0.0151/0.00467) for the pristine and water-washed films are shown, respectively.

physical nature of the hopping-based conduction process in the thin film of the PEDT/PSS associate. Note that for similar d_{max} values the wider the conduction window, the lower is the density of an average cell in the conducting pathway. This density is directly related to the conductivity via particle size. Beside the connectivity, this size is the key factor determining the conductivity.

Results and Discussion

The conducting windows of both pristine and water-washed films in the shown density intervals consist of a continuous network of T particles. In both films, the percolation path is generated (Figure 1). The respective current-carrying core, the backbone, is distinguished from the remaining "dead ends" (see above). The backbone connects all the sites on one face of the cube with these on the opposite face. In both films, the density of the backbone is ca. 3 times lower than that of the whole infinite cluster.

In agreement with the experiment, the shown characteristics of the water-washed film are only slightly different from those of the pristine film: the field density is higher, the density interval; i.e. the window is narrower, and the p_c value is lower. However, in the water-washed film, the density of the backbone is ca. twice lower. This points to the shortest pathway and more effective use of the conducting volume fraction in the latter film. These differences can be related to the higher conductivity of the water-washed film as evidenced by the experiment (see Introduction). In the light of recent work by Nardes et al.[25] (mass ratio 1/6 is used), in the present study obviously the percolating pathways are generated in the plane parallel to the substrate surface (the lateral conductivity).

Thus, the values of p_c, $P(p)$, and $P(p)_b$ serve as a measure of the efficiency of an infinite cluster.

The observed p_c values are below 0.1 (Figure 2). Because of the finite size of our sample (and also due to the fact that we had only one sample at hand for each parameter set), this number may slightly deviate from the asymptotic value. However, such

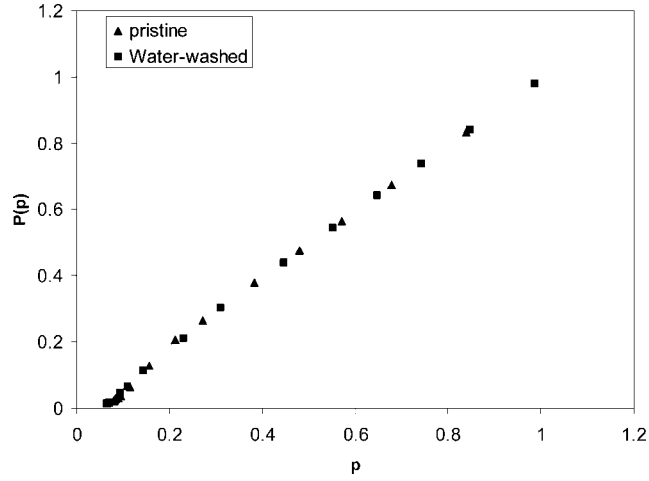

Figure 2. $P(p)$ vs p plot for pristine and water-washed films.

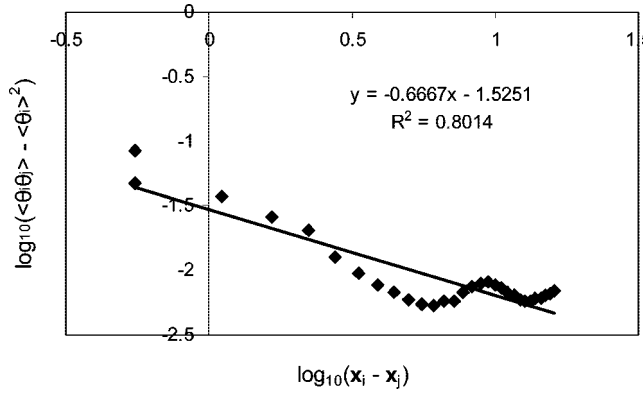

Figure 3. Calculation of the correlation function exponent H value for the pristine film. For the water-washed film the equation $y = -0.8833x - 2.0279$, $R^2 = 0.8974$ is calculated analogously. It should be stressed that the result $H \approx -0.44$ is approximate. Indeed, the scaling range is relatively narrow, and hence the finite-size effects may interfere; also, due to the limitations of the software package, only one set of density fields was generated for each parameter set, and hence the statistical uncertainties are high.

a deviation solely cannot explain the departure from the generally accepted value, 0.14−0.16, observed for the 3D lattice (irrespective of its symmetry) and for the continuum percolation including the metal−insulator transitions as well.[26] In proton conducting membranes, the p_c value is slightly lower, ca. 0.11−0.14.[2] Furthermore, surprisingly enough, in the region close to the threshold, the expected infinite slope, which classically signals the appearance of the percolation path and the disorder to order transition, is not observed. Instead, a nearly directly proportional dependence is seen. This cannot be ascribed solely to the finite-size effects because these would affect mostly the behavior at the smallest values of $P < 0.05$, and the continued trend would be observable for moderate values of P. The plot $P(p)$ vs y shows a similar linear relationship.

The conductivity behavior near the percolation threshold and the low p_c values are indicative of the presence of strong positive long-range correlations between the cells which tend to decrease the p_c level. Indeed, this is the case (Figure 3).

The correlation between the conducting sites is characterized by the occupation correlation function[21] defined as

$$c_\theta(\mathbf{x}_i - \mathbf{x}_j) = \langle(\theta_i - p)(\theta_j - p)\rangle \quad (1)$$

where $\mathbf{x}_i$ designates the position vector of a site and θ_i characterizes the state of the site; i.e., it is unity at a conducting

site and zero at nonconducting site. This function decays as a the power law at long distances $c_\theta(\mathbf{x}_i - \mathbf{x}_j) \propto |\mathbf{x}_i - \mathbf{x}_j|^{2H}$. From this follows

$$c_\theta(\mathbf{x}_i - \mathbf{x}_j) = \langle\theta_i\theta_j\rangle - \langle\theta\rangle^2 \propto |\mathbf{x}_i - \mathbf{x}_j|^{2H} \quad (2)$$

The average value of $\langle\theta_i\rangle$ is equal to the occupation probability p (equal to the volume fraction above). The criterion of the relevance of correlations is given as

$$-\frac{1}{\nu} < H < 0 \quad (3)$$

where ν is the critical exponent for the correlation radius (the average size of the largest finite cluster) in 3D is equal to 0.82 and H is an exponent calculated from eq 2.

We observe the values of the exponent H in the range of -0.34 to -0.44; while these results are not very accurate (see Figure 3), they are clearly higher than $-1/0.82 = -1.2$; this demonstrates the expected significance of the correlations, i.e., θ_i values are not independent of each other. We believe that the observed correlation is a logical result reflecting the connectedness of the conducting particles.

In conclusion, we have demonstrated that the presence of the correlated percolation threshold in the PEDT/PSS complex at an exceptionally low volume fraction of the PEDT particles is possible. In agreement with the experiment, the comparison of the percolation pathways in the pristine and water-washed films is indicative of the higher conductivity of the latter film.

How do these results depend on the PEDT/PSS mass ratio and on the doping level, and what is their contribution to the understanding of the overall conductivity under study? These questions have been addressed in the report of authors on the CISSE2008Online conference (Dec 2008).

The authors believe the methodology described to be useful in the investigation of the morphology of electronically conducting polymers in general.

Acknowledgment. The authors are grateful to the Estonian Science Foundation for financial support (Grants 6633 and 6121) and to the Accelrys Support Group for customizing computational programs.

References and Notes

(1) Kim, J. S.; Jackman, R. J.; Eisenberg, A. Filler and Percolation Behavior of Ionic Aggregates in Styrene-Sodium Methacrylate Ionomers. *Macromolecules* **1994**, *27*, 2789–2803.
(2) Edmondson, C. A.; Fontanella, J. J. Free volume and percolation in S-SEBS and fluorocarbon proton conducting membranes. *Solid State Ionics* **2002**, *152−153*, 355–361.
(3) Van Vlimmeren, B.; Maurits, N.; Zvelindovsky, A.; Sevink, G.; Fraaije, J. Simulation of 3D mesoscale structure formation in concentrated aqueous solution of the triblock polymer surfactants. Application of dynamic mean-field density functional theory. *Macromolecules* **1999**, *32*, 646–656.
(4) Staufer, D.; Aharony, A. *Introduction to Percolation Theory*, 2nd ed.; Taylor & Francis: Oxford, 1994.
(5) Kirchmeyer, S.; Reuter, K. Scientific importance, properties and growing applications of poly(3,4-ethylenedioxythiophene). *J. Mater. Chem.* **2005**, *15*, 2077–2088.
(6) Xing, K. Z.; Fahlman, M.; Chen, X. W.; Inganas, O.; Salaneck, W. R. The electronic structure of poly(3,4-ethylene-dioxythiophene): studied by XPS and UPS. *Synth. Met.* **1997**, *89*, 161–165.
(7) Ghosh, S.; Inganas, O. Self-assembly of a conducting polymer nanostructure by physical crosslinking: applications to conducting blends and modified electrodes. *Synth. Met.* **1999**, *101*, 413–416.
(8) Aasmundtveit, K. E.; Samuelsen, E. J.; Pettersson, L. A. A.; Inganas, O.; Johansson, T.; Feidenhans'l, R. Structure of thin films of poly(3,4-ethylenedioxythiophene). *Synth. Met.* **1999**, *101*, 561–564.
(9) Greczynski, G.; Kugler, Th.; Keil, M.; Osikowicz, W.; Fahlman, M.; Salaneck, W. R. Photoelectron spectroscopy of thin films of PEDOT-PSS conjugated polymer blend: a mini-review and some new results. *J. Electron Spectrosc. Relat. Phenom.* **2001**, *121*, 1–17.
(10) Niu, L.; Kvarnström, C.; Fröberg, K.; Ivaska, A. Electrochemically controlled surface morphology and crystallinity in poly(3,4-ethylenedioxythiophene) films. *Synth. Met.* **2001**, *122*, 425–429.
(11) Pettersson, L. A. A.; Ghosh, S.; Inganas, O. Optical anisotropy in thin films of poly(3,4-ethylenedioxythiophene)-poly(4-styrenesulfonate). *Org. Electron.* **2002**, *3*, 143–148.
(12) Kim, W. H.; Kushto, G. P.; Kim, H.; Kafafi, Z. H. Effect of annealing on the electrical properties and morphology of a conducting polymer used as an anode in organic light-emitting devices. *J. Polym. Sci., Part B* **2003**, *41*, 2522–2528.
(13) Zykwinska, A.; Domagala, W.; Czardybon, A.; Pilawa, B.; Lapkowski, M. In situ EPR spectroelectrochemical studies of paramagnetic centres in poly(3,4-ethylenedioxythiophene) (PEDOT) and poly(3,4-butylenedioxythiophene) (PBuDOT) films. *Chem. Phys.* **2003**, *292*, 31–45.
(14) Jonsson, S. K. M.; Birgerson, J.; Crispin, X.; Greczynski, G.; Osikowicz, W.; Denier van der Gon, A. W.; Salaneck, W. R.; Fahlman, M. The effects of solvents on the morphology and sheet resistance in poly(3,4-ethylenedioxythiophene)-polystyrenesulfonic acid (PEDOT-PSS) films. *Synth. Met.* **2003**, *139*, 1–10.
(15) Crispin, X.; et al. Conductivity, morphology, interfacial chemistry, and stability of poly(3,4-ethylene dioxythiophene)-poly(styrene sulfonate): A photoelectron spectroscopy study. *J. Polym. Sci., Part B* **2003**, *41*, 2561–2583.
(16) Timpanaro, S.; Kemerink, M.; Touwslager, F. J.; De Kok, M. M.; Schrader, S. Morphology and conductivity of PEDOT/PSS films studied by scanning-tunneling microscopy. *Chem. Phys. Lett.* **2004**, *394*, 339–343.
(17) Kemerink, M.; Timpanaro, S.; deKok, M. M.; Meulemkamp, E. A.; Touwslager, M. J. Three-dimensional inhomogeneities in PEDOT: PSS films. *J. Phys. Chem. B* **2004**, *108*, 18820–18825.
(18) De Kok, M. M.; et al. Modification of PEDOT:PSS as a hole injection layer in polymer LEDs. In *Physics of Organic Semiconductors*; Brütting, W., Ed.; Wiley-VCH: Berlin, 2005; pp 451−473.
(19) Smith, R. R.; Smith, A. P.; Stricker, J. T.; Taylor, B. E.; Durstock, M. F. Layer-by-layer assembly of poly(ethylenedioxythiophene): poly(styrenesulfonate). *Macromolecules* **2006**, *39*, 6071–6074.
(20) DeLongchamp, D. M.; Vogt, B. D.; Brooks, C. M.; Kano, K.; Obrzut, J.; Richter, C. A.; Kirillov, O. A.; Lin, E. K. Influence of a water rinse on the structure and properties of poly(3,4-ethylene dioxythiophene):poly(styrene solfonate) films. *Langmuir* **2005**, *21*, 11480–11483.
(21) Isichenko, M. B. Percolation, statistical topography, and transport in random media. *Rev. Mod. Phys.* **1992**, *64*, 961–1033.
(22) Kaevand, T.; Öpik, A.; Lille, Ü. A mesoscale simulation of the morphology of the PEDT/PSS complex in the water dispersion and thin film: the use of the MesoDyn simulation code. Sobh, T. *Advances in Computer and Information Science and Engineering*; Springer: Berlin, 2008; Vol. *XVIII*, pp 540−546. Online access at http://www.springerlink.com/content/ht658j2j817x834h/.
(23) Fraaije, J. G. E. M.; van Vlimmeren, B. A. C.; Maurits, N. M.; Postma, M.; Evers, O. A.; Hoffmann, C.; Altevogt, P.; Goldbeck-Wood, G. The dynamic mean-field density functinal method and its application to the mesoscopic dynamics of quenched copolymer melts. *J. Chem. Phys.* **1997**, *106*, 4260–4269.
(24) Nicolaides, D. Mesoscale modelling. *Mol. Simul.* **2001**, *26*, 51–72.
(25) Nardes, A. M.; Kemerink, M.; Janssen, R. A.; Bastiaansen, J. A.; Kiggen, M. M.; Langeveld, B. M.; van Breemen, J. J.; de Kok, M. M. Microscopic understanding of the anisotropic conductivity of PEDT: PSS thin films. *Adv. Mater.* **2007**, *19*, 1196–1200.
(26) Zallen, R. *The Physics of Amorphous Solids*; John Wiley Sons: New York, 2004.

MA802160X